Multi-radio Data Fusion for Indoor Localization using Bluetooth and WiFi

Afaz Uddin Ahmed[1,2][a], Reza Arablouei[1][b], Frank de Hoog[1][c],
Branislav Kusy[1][d] and Raja Jurdak[1,2][e]

[1]*School of Information Technology and Electrical Engineering, University of Queensland, St. Lucia, QLD 4072, Australia*
[2]*Data61 Group, CSIRO, QLD 4069, Australia*

Keywords: Data Fusion, Multi-radio, Indoor Localization, WiFi, Channel State Information, Bluetooth Low Energy.

Abstract: Location estimation through fusing the information obtainable from multiple radio systems can reduce the dependency on each system and improves the performance. Research on fusion-based indoor localization using WiFi and Bluetooth-low-energy (BLE) beacons has mostly been limited to training-based approaches. In this paper, we propose a training-free indoor localization technique using received signals from WiFi and BLE device. The proposed technique estimates the position of the user device by fusing the information that it gains regarding the position of the target from the WiFi channel state information (CSI) and the RSSI measurements of BLE beacons. We use the WiFi CSI to estimate the angle of arrival (AoA), which we then use in conjunction with the RSSI measurements from the BLE beacons to develop a multi-radio fusion framework for indoor localization. We use a weighted centroid localization method to obtain an initial position estimate from the RSSI measurements. The initial position estimation helps to resolve the ambiguities in the AoA. The proposed technique is based on maximum-likelihood estimation (MLE) exploiting the probability density functions of the estimated AoA and the RSSI-induced distances. Simulation results show that the proposed technique improves the localization accuracy by 30% in a typical indoor environment compared with previous approaches.

1 INTRODUCTION

Indoor localization using measurements from multiple wireless platforms offers better reliability for location-based applications compared to a single wireless platform (Kanaris et al., 2017). Fusing measurements from multi-radio systems compensate for the limitations of the individual platforms such as inconsistency in the measurements, the randomness of the measured data due to noise from the environment, high computational complexity, and high duty cycle. Integration of measurements from multiple platforms improves the reliability and accuracy of the localization system. It reduces the error in location estimation and performs better than the stand-alone system (Hilsenbeck et al., 2014).

[a] https://orcid.org/0000-0002-9919-3126
[b] https://orcid.org/0000-0002-6932-2900
[c] https://orcid.org/0000-0002-4632-564X
[d] https://orcid.org/0000-0001-9082-3243
[e] https://orcid.org/0000-0001-7517-0782

Data fusion for user localization was initially introduced by fusing the GPS and inertial sensors data from the smart-phone for outdoor tracking (Qi and Moore, 2002). The main purpose was to make the localization process more energy efficient by reducing the duty cycle of the GPS unit. This is feasible because even if the GPS signal gets interrupted at a regular interval, data collected from the inertial sensors can aide the localization process through a data fusion framework. Multi-radio-fusion-based localization is a new branch in indoor localization but is challenged by the random fluctuation of signal strength.

Past fusion based indoor localization techniques were developed on platforms such as, Bluetooth (Mirowski et al., 2013), WiFi (Leppäkoski et al., 2013; Lim et al., 2007), ultra-wide-band (Gezici et al., 2005), or ultrasound (Kuban et al., 2005) in conjunction with pedestrian dead reckoning (PDR) (Fang et al., 2005; Chang et al., 2015). PDR is a process to use smart-phones inertial sensors, accelerometers, magnetometers, and gyroscopes to determine the current position based on the previous positions

13

recorded. The initial data fusion for indoor localization integrates the data from WiFi and PDR (Evennou and Marx, 2006). Fusion using data from inertial measurement units (IMU) is widely used in recent indoor fusion based techniques (Chen et al., 2014; Koo et al., 2014; Li et al., 2017; Gallagher et al., 2012; Lin et al., 2015). In (Liu et al., 2017), a multi-sensor fusion method is proposed using cameras, WiFi, and IMU measurements. Use of cameras for indoor localization is also proposed in (Papaioannou et al., 2014; Jiao et al., 2018; Gu et al., 2017). For indoor navigation of robots, different heuristic fusion algorithms have been developed using RFID tags (Choi et al., 2011), ultrasonic sensors (Luo and Lai, 2012), piezoelectric sensors (Luo and Chen, 2013), and positioning radar (Dobrev et al., 2016). Past researches tend to characterize the PDR as a non-linear function and leverage particle filters to tackle the non-linearity. In the measurements of PDR, several parameters need to be specified, including the initial point and walking direction (Tarrío et al., 2011). However, the high computational load of applying particle filters in radio mapping techniques necessitates offline tracking (Gustafsson et al., 2002). In recent times, there have been a few fusion-based techniques that use both bluetooth low energy (BLE) and WiFi. These techniques use the received signal strength indicator (RSSI) measurements from both BLE and WiFi to execute the training-based and training-free models. Fusing RSSI from two different wireless devices improves the localization performance, but the performance is still limited by the random fluctuation of the RSSI measurements. Moreover, these techniques do not take advantage of the recently available resource, such as CSI measurement from the WiFi. In section 2, we briefly discuss CSI based techniques.

With the growing need for location-based applications, there is a demand for a universal and easily deployable indoor localization system. In this research, we propose a multi-radio data fusion framework for indoor localization using BLE and WiFi access point. A BLE beacon is an easily-deployable low-cost wireless sensor device that supports a wide range of indoor localization techniques. However, position estimation using BLE beacon has a high error rate due to RSSI fluctuations. Nowadays, WiFi access points are wide availability in indoor premises and have the potential to resolve the fluctuation of RSSI in fusion-based localization. In recent times, the channel state information (CSI) received at the WiFi access point is easily accessible in some commercial network interface card (NIC). CSI contains the information of the channel impulse response, which is influenced by the channel characteristics, including multipath propaga-

tion. CSI-based localization techniques are complicated but more accurate and reliable than RSSI based techniques (Kotaru et al., 2015). However, most CSI-based techniques require the user device to connect with multiple WiFi access points for localization purposes. It is challenging to get connected to multiple access point in residential places where access to most of the networks is password protected. In the case of indoor commercial space, proper RF site survey does not allow a densely overlapping zone of the same network. Moreover, the user device periodically switches connection among WiFi access points to provide CSI measurement to assist the localization process. Not only this hinders the internet connectivity of the device, but it also creates network instability as the devices will continuously disconnect and reconnect.

In this work, we fuse the RSSI measurements from BLE beacons and the CSI measurements from WiFi to develop a new indoor localization technique. The localization technique focuses on the easily deployable feature of BLE beacon and CSI based angle of arrival (AoA) estimation technique at WiFi access points. The proposed fusion framework combined the existing RSSI technique with AoA estimation from WiFi and obviates the deployment of multiple WiFi access points. The CSI data from the WiFi is fed into the modified matrix pencil (MMP) method developed in (Ahmed et al., 2018). The MMP is a sub-space based high-resolution direction-of-arrival (DoA) estimation technique which works with the CSI data. It estimates the AoA and time of flight (ToF) of the incoming signal. ToF estimation from CSI data is not reliable. Previous works have used multiple WiFi access points to estimate the position using triangulation (Kotaru et al., 2015). In our fusion framework, we use only one WiFi access point. Use of just one WiFi access point to implement the existing techniques is challenging. The estimated AoA contains three ambiguities. In the paper, we eliminate these ambiguities by estimating an initial position using weighted centroid localization (WCL). WCL is a weight based range-free technique that estimates a position using weights which are propositional to the magnitude of the RSSI (Blumenthal et al., 2007; Chan and Soong, 2016; Laurendeau and Barbeau, 2009). The range-free technique does not calculate the distance between the transmitters and receivers (Karim et al., 2010). We use the lognormal shadowing pathloss model to estimate the distances using the BLE RSSI and then develop a fusion technique using the estimated-distance, and estimated-AoA. The proposed fusion technique is called distance-AoA fusion, and it fuses the probability density functions (PDF) of

estimated-distance and estimated-AoA. We also compare the results with a similar fusion technique using BLE and WiFi proposed in (Galván-Tejada et al., 2013). The technique uses multilateration technique using the RSSI from both BLE and WiFi without using radio-mapping.

2 RELATED WORKS

A BLE and WiFi-based fusion technique is presented in (Aparicio et al., 2008) that uses RSSI measurement from both platforms. The proposed method creates two sets of radio-maps using the RSSI measurement from BLE and WiFi. The tracking area is divided into crown-shaped regions by considering different thresholds for RSSI values. In the fusion part, a crown-shaped region is selected initially using the Bluetooth radio-map. The WiFi radio-map is used for the final position estimation inside the target zone. The average error reported is approximately 2.32 meters. A similar RSSI based technique is proposed in (Aparicio et al., 2009) that uses RSSI from both WiFi and BLE for fingerprinting. The technique calculates the absolute difference of WiFi RSSI and BLE RSSI for each position. It calculates the mini-max distance between the points. Then the distance is calculated by averaging the three nearest neighbors co-ordinates and weights which are inversely proportional of the distances among them. The reported error in the technique is 2.21 meter. Another technique has been presented in (Kanaris et al., 2017) that uses RSSI from the WiFi to create the radio-map. The RSSI from the BLE is used to calculate the distance from a particular BLE. Then, adding and subtracting a fixed tolerance with the distance, two circles are drawn from BLE position. It creates a doughnuts shape region inside the mapping area. The final position is estimated by looking at the WiFi fingerprints inside the doughnut-shaped region. The average position error is reported to be 4.05 meters for 12 test points. A training-free fusion technique is presented in (Galvan-Tejada et al., 2012) which performs multilateration using RSSI-distance equations. RSSI from WiFi and BLE gives an estimation of distance which is used in multilateration. In the analysis of the simulations, 400 iterations are performed with setups having 3 WiFi and 1 BLE, 3 WiFi - 2 BLE, and 3 WiFi-5 BLE. The result shows that 45% of the estimation have a position error of less than 1.839 meters. A similar approach is used in (Galván-Tejada et al., 2013) where a regression model is developed using RSSI from 10 points ranging distances from 0.5 to 5 meter. The model is used to estimate the distance from the RSSI.

The fusion technique uses a minimum of 8 equations using RSSI from WiFi and BLE, and then the least square solution is performed to estimate the final position. For 30 measurements in three locations, the lowest total error achieved is 0.87 meters. Table 1 briefly shows work discussed above.

In previous research, WiFi and BLE are used for RSSI based radio mapping/fingerprinting. Some of the training-free techniques use the pathloss model to estimate the distance. Fingerprinting techniques are confined to indoor location, and the resolution of the mapping dataset has an impact on the estimation performance (Evennou and Marx, 2006). The process requires a pre-profiling stage that requires an offline session to create a dataset for indoor-locations. The training process limits the easily deployable feature of the training-based system. Moreover, any change or movement of the furniture invalidates the offline training data. On the other hand, the training-free technique calculates distances using a path loss model to estimate location using multilateration. The technique is independent of pre-profiling stage and uses the RSSI from both BLE and WiFi. To the best of our knowledge, till to-date, no fusion based framework has used the CSI measurements. In this research, we present an indoor location system that fuses the CSI collected from a WiFi access point and the RSSI measurements from multiple BLE beacons. Our goal is to develop a cost-effective system using easily deployable wireless device and BLE beacons. The closest comparable technique discussed to ours is presented (Galván-Tejada et al., 2013), uses RSSI measurements from both WiFi and BLE. It is a training-free technique that calculates the distance from RSSI. The lowest mean position errors it reports at three different points in an area surrounded by the BLE and WiFi are 0.869 meters, 1.0112 meters, and 2.326 meters. In the result section, we implement the technique in the simulation and compare it with our proposed fusion techniques.

3 SYSTEM OVERVIEW

In the proposed multi-radio fusion-based localization, we use two properties of the incoming signals from two different wireless platforms the CSI of the received signal at the WiFi access point and RSSI measurements at the user device. The CSI and RSSI values are sent to the cloud through the WiFi access-point to perform the indoor localization. The user learns the position through a smart-phone app connected to the cloud.

Table 1: Related works.

Article	Year	Bluetooth	WiFi	Radio Map	Fusion	Error
A Fusion Based on Bluetooth and WLAN Technologies for Indoor location(Aparicio et al., 2008).	2008	Radio-map using RSSI.	Radio-map using RSSI.	Required.	Fingerprint matching.	2.32 meter.
An Indoor Location Method Based on a Fusion Map using Bluetooth and WLAN Technologies (Aparicio et al., 2009).	2009	Radio-map using RSSI.	Radio-map using RSSI.	Required.	Fingerprint matching.	2.21 meter.
WiFi Bluetooth based combined positioning algorithm (Galvan-Tejada et al., 2012).	2012	Distance form RSSI.	Distance form RSSI.	Not required.	Multilateration.	45% results has less than 1.839 meter error.
Bluetooth-WiFi based combined positioning algorithm, implementation and experimental evaluation (Galván-Tejada et al., 2013).	2013	Distance from RSSI.	Distance from RSSI.	Not required.	Least square solution.	Lowest total error is 0.87 meter.
Fusing Bluetooth Data with WiFi Radio-maps for Improved Indoor Localization (Kanaris et al., 2017).	2017	Distance form RSSI.	Radio-map using RSSI.	Required.	Fingerprint matching.	Average 4.05 meter for 12 test points.

3.1 WiFi

In a previous study, a fast algorithm has been developed to estimate the AoA and ToF of the multi-path signals using the CSI values at the WiFi access point (Ahmed et al., 2018). The algorithm uses an updated version of the high-resolution DoA estimation algorithm, called the modified matrix pencil (MMP). It significantly outperforms the 2D MUSIC (multiple signal classification) algorithms used in (Kotaru et al., 2015) by estimating the AoA and ToF at least 200 times faster. In both techniques, the high-resolution algorithms are fed with CSI measurements in a modified matrix format. However, in 2D MUSIC it creates a 2D grid of MUSIC spectrum to find the peaks that correspond to AoA-ToF pairs of the multipath signals. While in MMP, it performs two 1-dimensional solutions for AoA and ToF without creating any 2D grid. It also pairs the AoA and ToF by using eigen vector multiplication process. Both techniques provide an accurate estimation of the AoA with unreliable ToF. In the presence of noise and indoor multipath propagation, the estimation of ToF in nanosecond scale is very challenging mainly because of the presence of sampling-offsets and frequency-offsets in the commercial NICs. The differences between the subcarrier frequencies are very small, and distance traveled in indoor is also very short and do not create a significant difference in the phases of the subcarriers. However, the crude estimation of ToF helps to determine the correct AoA. The smallest ToF represents the signal traveling in the direct path, although

it is not equal to the travel time of the signal (Kotaru et al., 2015). In a uniform array antenna, the estimated AoA is called the projected AoA. If the antennas are placed horizontally, the estimated AoA becomes the vertical projection. The estimated AoA on a uniform antenna array contains an array ambiguity (Gazzah and Delmas, 2012). At the receiver, the carrier phase measurements are generated using a frequency lock loop (FLL). The FLL matches the frequency of the received and the transmitted signals. The measurement of the phase in CSI has a modulo of π, which leads to another type of ambiguity, called the phase ambiguity (Jacobs and Ralston, 1981; Teunissen, 2003). In our fusion-based localization, we resolve these ambiguities in the estimated AoA by using the initial position estimate given by the WCL.

3.2 Bluetooth

In the BLE network, we perform an initial position estimation using the RSSI measurements from multiple BLE beacons. The initial position of the user is estimated using the WCL technique. For the fusion technique, we estimate the distance between the receiver and the BLE beacons using the log-normal shadowing pathloss model (Büyükçorak et al., 2015). In the log-normal shadowing model, the distribution of RSSI is approximated by a Gaussian in the logarithmic domain (Zanca et al., 2008; Ergen et al., 2014; Yiu et al., 2016).
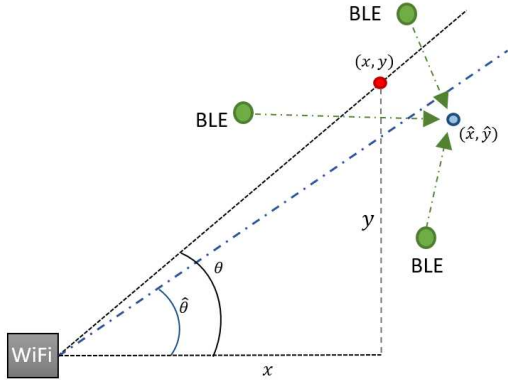
Figure 1: The true AoA and target position, the AoA estimated from WiFi CSI, and the target position estimated from BLE beacon RSSIs.

3.3 Fusion

We use the estimated AoA and RSSI measurements in the fusion model development. The steps in the fusion model development are mentioned below.

3.3.1 Step 1

In the first step, we resolve the array and phase ambiguities in the estimated AoA. The estimated AoA has three ambiguities. For an estimated AoA, θ, the phase-periodic ambiguity is $\pi \pm \theta$ and the phase-symmetric ambiguity is $\pm \theta$. The phase-periodic ambiguity also has its symmetric ambiguity. These AoA ambiguities are resolved with the help of the initial position estimation using WCL. We select the angle for AoA that creates the least difference with the angle of the initial position estimate.

3.3.2 Step 2

In the second step, we use the AoA and RSSI measurements to develop a fusion technique based on maximum-likelihood estimation. To this end, we maximize the product of the PDFs of the RSSI-induced distances and the estimated AoA.

We model the PDF of the AoA as Gaussian. The approximation is based on a simulation analysis discussed in the next section. To evaluate the fusion technique, we consider two choices for the variance of the AoA, the theoretical value based on the Cramer-Rao lower bound (CRLB), and the measured value. The CRLB gives the minimum achievable variance for any unbiased estimator. The unbiased variance is least noisy and in this study we use the CRLB variance to test the performance of the fusion technique. We also calculate the measured variance through simulations with known position and AoA.

4 MULTI-RADIO FUSION ARCHITECTURE

4.1 PDF of BLE RSSI

Let us consider q BLE beacons deployed in an area having the same height as the target node. The target node and the BLE beacons have isotropic antennas. The set of BLE beacons is $U = \{A_1, A_2, \cdots, A_q\}$. The 2-D locations of the BLE beacons are known and the location set is $u = \{a_1, a_2, \cdots, a_q\}$, where $a_i = (x_i, y_i)$. Let the position of the target node be $b = (x, y)$. Let $R_i(dBm)$ be the RSSI of the ith beacon at the target node without any noise, i.e. $R_i(dBm) = 10\log_{10}R_i$. The symbol $R_i(dBm)$ represents the RSSI in decibel-milliwatt and R_i in milliwatt. At any given time, the target node receives signals from p number of BLE beacons. The active set of BLE beacons is $V \subseteq U$. The goal is to estimate the position of the target node b.

The measured RSSI from the ith beacon is $\tilde{R}_i(dBm)$, which includes noise. The noise in $\tilde{R}_i(dBm)$ is additive zero-mean Gaussian with standard deviation (STD) σ_{R_i}. Therefore, we have

$$\tilde{R}_i(dBm) = R_i(dBm) + n_{R_i}$$

$$n_{R_i} \sim \mathcal{N}(0, \sigma_{R_i}^2).$$

RSSI distance measurement uses the logarithmic distance path-loss model (Golestani et al., 2014; Nowak et al., 2016; Nguyen et al., 2011). It is expressed as

$$\tilde{R}_i(dBm) = R_0(dBm) - 10\eta_p log_{10}(d_i/d_0) + n_{R_i} \quad (1)$$

here $d_i = \sqrt{(x-x_i)^2 + (y-y_i)^2}$, and $R_0(dBm)$ is the power received at a reference distance d_0. The parameter η_p is the pathloss co-efficient that depends on the environment. In most cases, η_p is estimated from the prior measurements. The PDF of the RSSI measurement from the ith BLE is:

$$p(\tilde{R}_i(dBm)) = \frac{1}{\sqrt{2\pi}\sigma_{R_i}} e^{-\frac{(\tilde{R}_i(dBm) - R_i(dBm))^2}{2\sigma_{R_i}^2}} \quad (2)$$

Substituting (1) into (2) gives

$$p(\tilde{d}_i) = \frac{\xi}{d_i\sqrt{2\pi}\sigma_{R_i}} e^{\left[-\frac{v}{8}\left(\log\frac{d_i^2}{\tilde{d}_i^2}\right)^2\right]}. \quad (3)$$

here $\xi = 10/\ln 10 = 4.3429$, $v = \left(\frac{10\eta_p}{\sigma_{R_i}\ln 10}\right)^2$, $\tilde{d}_i$ is the distance calculated from $\tilde{R}_i(dBm)$.

4.2 Weighted Centroid Localization

We use the WCL to calculate the initial values of x and y. The WCL is a localization technique that estimates the position by assigning weights to each BLE beacon and taking the weighted average of their RSSI values. The weightes are assigned based on the technique discussed in the literature review (Blumenthal et al., 2007). The estimated position of the target node is given by the WCL algorithm considered:

$$x_0 = \frac{\sum\limits_{i=1}^{p} w_i x_i}{\sum\limits_{i=1}^{p} w_i},$$

$$y_0 = \frac{\sum\limits_{i=1}^{p} w_i y_i}{\sum\limits_{i=1}^{p} w_i}.$$

here w_i is the assigned weight for the ith BLE beacon.

4.3 PDF of WiFi AoA

Let us consider that the target node is connected to a WiFi access point and sends a signal in the uplink. Let τ and θ be the ToF and AoA of the uplink signal. The WiFi access point has three antennas separated by a distance l, and each of the antennas receives n narrow-band signals, one for each of the subcarriers whose frequencies are separated by δ. WiFi uses OFDM (orthogonal frequency-division multiplexing) modulation, where the signal gets divided into multiple narrow-band signals and transmitted over the channel. Let us denote the CSI value of the subcarrier with the lowest frequency on the first antenna by the complex number γ. It then follows that the CSI value of the sth subcarrier received at the ath antenna is $\gamma g^{a-1} h^{s-1}$ where $g = \exp\left(2\pi j l \lambda^{-1} \sin\theta\right)$ and $h = \exp(2\pi j \delta\tau)$. Let $f_\theta = l\lambda^{-1}\sin\theta$, which gives $g = \exp(2\pi j f_\theta)$. Let ρ and ψ be the amplitude and phase of γ, respectively. Let us assume that there is only one line-of-sight signal, and the multipath signals are weak and do not effect the CSI measurements. The work on CSI based AoA estimation proposed earlier shows the procedure of finding the real AoA of the target user in case there a multipath dominating multi paths affecting the CSI measurements (Ahmed et al., 2018). Here, for simplicity, we assume there is only one existing AoA in the CSI measurements. Using MMP, we estimate the AoA of the uplink signal. The CSI values associated with all three antennas and n sub-carriers for only one

incoming signal can be collected in the CSI matrix as

$$C' = \begin{bmatrix} 1 \\ g \\ g^2 \end{bmatrix} \gamma \begin{bmatrix} 1 & h & \cdots & h^{n-1} \end{bmatrix}.$$

Let us assume N_w be the environment noise. N_w has a dimension of $(3 \times n)$. Therefore, noisy CSI can be expressed as

$$C = C' + N_w.$$

In the previous research in (Ahmed et al., 2018), this C' matrix is used to estimate the AoA and ToF of the incoming signals, including multipath. The article also discusses the technique to differentiate the line of sight or direct path signal using the ToF estimation. The presence of multipath signals inside the CSI dataset results in multiple AoAs. The shortest ToF represents the line-of-sight or the direct-path signal.

We assume that the estimation of AoA is unbiased. In the next section, it is shown that the empirical distribution of estimated AoA in a noisy environment is very close to Gaussian. Therefore, the PDF of the estimated AoA is

$$p(\theta) = \frac{1}{\sqrt{2\pi}\sigma_\theta} \exp\left(-\frac{(\theta - \hat{\theta})^2}{2\sigma_\theta^2}\right). \qquad (4)$$

here σ_θ is the STD and $\hat{\theta}$ is the estimated mean of AoA. The STD of the AoA is calculated from a number of estimated AoAs at known angles. We assume the WiFi access point is positioned at the origin and $\theta = \tan^{-1}\left(\frac{y}{x}\right)$.

4.4 Fusion Technique

Let us assume that the errors for AoA and distance are independent. The log likelihood function of the product of distance and AoA PDFs given in (3) and (4) is,

$$\begin{aligned} L(x,y) = & \ln\left(\frac{1}{\sqrt{2\pi}\sigma_\theta} \exp\left(-\frac{\left(\tan^{-1}\left(\frac{y}{x}\right) - \hat{\theta}\right)^2}{2\sigma_\theta^2}\right)\right) \\ & + \sum_{i=1}^{p} \ln\left(\frac{\xi}{\sigma_{\tilde{R}_i}\sqrt{2\pi((x-x_i)^2 + (y-y_i)^2)}} \right. \\ & \left. \exp\left[-\frac{v}{8}\left(\log\frac{d_i^2}{\tilde{d}_i^2}\right)^2\right]\right). \end{aligned}$$

$L(x,y)$ is twice continuously differentiable with respect to the variables. We estimate the values of (x,y)

by maximizing the function. Therefore, the optimization problem can be expressed as

$$
\max_{x,y} \left[\ln \left(\frac{1}{\sqrt{2\pi}\sigma_\theta} \exp \left(-\frac{\left(\tan^{-1}\left(\frac{y}{x}\right) - \hat{\theta}\right)^2}{2\sigma_\theta^2} \right) \right) \right.
$$
$$
\left. + \sum_{i=1}^{p} \ln \left(\frac{\xi}{d_i\sqrt{2\pi}\sigma_{\tilde{R}_i}} e^{\left[-\frac{y}{8}\left(\log \frac{d_i^2}{\tilde{d}_i^2} \right)^2 \right]} \right) \right].
$$

The equation above is a nonlinear optimization problem without any constraints. We calculate first and second order derivatives to find the value of x and y that maximizes the equation.

We determine the Hessian matrix of $L(x,y)$. The Hessian matrix is (see Appendix A)

$$
\nabla^2 L = \begin{bmatrix} \frac{\partial^2 L}{\partial x^2} & \frac{\partial^2 L}{\partial y \partial x} \\ \frac{\partial^2 L}{\partial x \partial y} & \frac{\partial^2 L}{\partial y^2} \end{bmatrix}
$$

We use the Newton's algorithm to solve the above problem. At each iteration of the algorithm, we solve the following system of linear equations:

$$
\begin{pmatrix} \frac{\partial^2 L}{\partial x^2} & \frac{\partial^2 L}{\partial y \partial x} \\ \frac{\partial^2 L}{\partial x \partial y} & \frac{\partial^2 L}{\partial y^2} \end{pmatrix} \begin{pmatrix} \delta x \\ \delta y \end{pmatrix} = \begin{pmatrix} \frac{\partial L}{\partial x} \\ \frac{\partial L}{\partial y} \end{pmatrix}
$$

here, L denotes the log-likelihood (objective) function. Then, the estimates are updated as $(\hat{x}, \hat{y}) \to (\hat{x} + \delta x, \hat{y} + \delta y)$. The iterations are continued until $(\delta x, \delta y)$ becomes small.

4.5 CRLB Calculation

The STDs σ_θ and $\sigma_{\tilde{R}_i}$ in $L(x,y)$ are the parameter known from prior measurements. It also can be calculated using some initial measurements. Change of STDs value also changes the accuracy of the location estimation. In this sub-section, we calculate the CRLB of the STDs using the known values of distances and AoA. The CRLB variance of (3) is the same as the minimum variance of noise n_{R_i}. Therefore, we write $\sigma_{R_i,cr}$ is the CRLB STD.

4.5.1 CRLB of WiFi AoA

In WiFi, the unknown parameters are γ, ϕ, θ and τ (see section 4.3). In practice, we only need the value of θ but for that we need to calculate the Fisher information matrix (FIM), which contains all the other unknown parameters. For the AoA estimation, the unknown parameter vector κ is:

$$
\kappa = [\gamma, \phi, \theta, \tau]^T.
$$

Therefore, the PDF of C' as in (Hua, 1992) is

$$
p(C'|\kappa) = \frac{1}{(2\pi\sigma_w^2)^{MN}} \exp\left(-\frac{1}{\sigma_w^2} ||C' - C||^2 \right)
$$

here $||.||$ donates the 2-norm, σ_w^2 is the variance of the noise, and κ is a $4I \times 1$ vector of unknown, I is the number 2-D sinusoids in the CSI dataset, M is the number of antenna elements, and N is the number of subcarriers. Hence, the log-likelihood function is:

$$
L(\kappa|C') = \ln(p(C'|\rho, \phi, \theta, \tau)).
$$

Therefore, the corresponding FIM is:

$$
F_{i,j} = -\mathrm{E}\left[\frac{\partial^2 L(C'|\kappa)}{\partial \kappa_i \partial \kappa_j} \right],
$$
$$
F_{ij} = \frac{2}{\sigma_w^2}\mathrm{Re}\left[\frac{\partial C'^H}{\partial \kappa_i} \frac{\partial C}{\partial \kappa_j} \right].
$$

here Re[.] denotes the real part, $F(\kappa)$ is a $4I \times 4I$ matrix and, F_{ij} is the (i,j)th entry of F.

In (Hua, 1992), the FIM has been derived for m antenna arrays and n subcarriers as (see Appendix B)

$$
F = \begin{bmatrix} F_{\rho\rho} & F_{\rho\phi} & F_{\rho\theta} & F_{\rho\tau} \\ F_{\rho\phi}^T & F_{\phi\phi} & F_{\phi\theta} & F_{\phi\tau} \\ F_{\rho\theta}^T & F_{\phi\theta}^T & F_{\theta\theta} & F_{\theta\tau} \\ F_{\rho\tau}^T & F_{\phi\tau}^T & F_{\theta\tau}^T & F_{\tau\tau} \end{bmatrix}. \tag{5}
$$

The square root of the third diagonal element of F^{-1} corresponds to the CRLB of AoA. Let $\sigma_{\theta,cr}$ be the CRLB STD of the estimated AoA.

Replacing σ_θ with $\sigma_{\theta,cr}$ in (4) gives:

$$
p(x,y) = \frac{1}{\sqrt{2\pi}\sigma_{\theta,cr}} \exp\left(-\frac{\left(\tan^{-1}\left(\frac{y}{x}\right) - \hat{\theta}\right)^2}{2\sigma_{\theta,cr}^2} \right). \tag{6}
$$

5 SIMULATION AND RESULTS

We develop a 2D model simulation model using MATLAB. The simulation model considers an area of 20m x 20m with 20 BLE beacons and one WiFi access point. The current setup of the simulation is considering 2D localization in a 2D plane. Azimuth angle for indoor localization is not that important and it does not have any significant effect in indoor positioning (Seong et al., 2019).

The WiFi access point is positioned in the center of the simulation area. The BLE beacons are randomly positioned with in the simulation area. The frequency band in WiFi is channel one in 2.4 GHz band. In an indoor environment, signal has 5-8 strong multipaths(Kotaru et al., 2015). In our simulation, we consider 5 multipaths in indoor environment. The
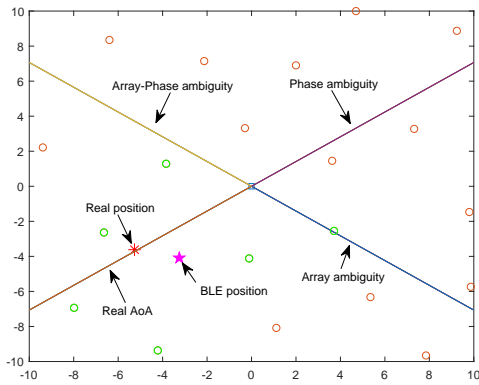
Figure 2: WiFi AoA estimation with ambiguity in the functioning area.

Figure 3: QQplot test.

magnitude of the multipath signal is obtained using 3D wireless prediction software - Wireless insite(wir,). The details of the simulation using Wireless-Insite is shown earlier research in (Ahmed et al., 2018). For every initial position estimation using WCL, we select six BLEs with the highest RSSI values. The simulation parameters are given in Table 2. Figure 2 shows the ambiguities of the estimated AoA and initial estimated position inside the simulation area.

Table 2: System Parameters.

Parameters/Variables	Properties
Area	20m x 20m
Number of BLE beacons	20
Number of BLE beacons used for localization	6
Frequency	2403.0225 MHz
Number of subcarrier	30
Number of WiFi antenna	3
Subcarrier spacing	0.630 MHz
SNR (WiFi)	15 dB
Number of Multi-path	5
Transmission Power	-12 dBm
Received power at 1 m distance	-77 dBm
Pathloss co-efficient, η_p	1.8
BLE std	3 dB

5.1 Distribution of Estimated AoA Error

We calculate the AoA estimation error for 10000 trails with a 15 dB signal to noise ratio (SNR). In each simulation, we randomly distribute the target node and calculate the noisy CSI data. All the simulations we performed having the target node at a 30-degree angle from the WiFi access point. Figure 3 QQ plot
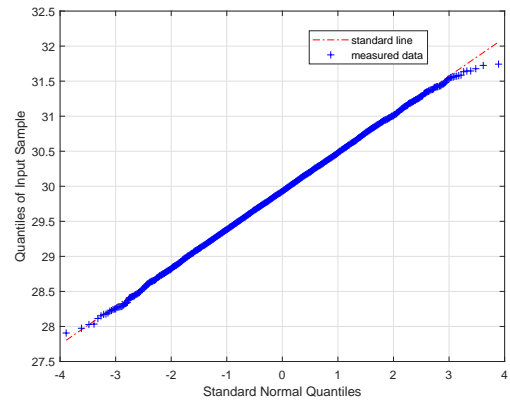
is a graphical method for comparing two probability distributions by plotting their quantiles against each other. Figure 3 illustrates that the distribution of the AoA is in good agreement with a normal distribution. The mean estimated AoA is 29.93-degree.

5.2 Performance of the Proposed Techniques

We ran 10000 independent trials using both the theoretical (CRLB) and measured variances. In each trial, the BLE beacon and target node positions are arbitrarily selected. We consider zero-mean Gaussian noise in the RSSI. Figure 4 shows the cumulative distribution function (CDF) of the position error using PDFs having four possible combination of CRLB and measured variances. From the figure, we can see that the proposed technique performs best with both PDFs having variances as measured variances. The root-mean-square-error (RMSE) of position with measured variances of 3.35-degree is 1.89 meters. Table 3 shows the estimated position error in meters as RMSE for different combinations of CRLB and measured variances in the PDFs. However, if we consider 80% of the estimation with higher accuracy, the fusion technique using CRLB variance in BLE PDF shows a better performance. It also performs better for position estimation with 3-meter error tolerance.

CRLB variance of AoA requires the values of ρ, ϕ, θ, and τ. In practice, it is not feasible to estimate the values of all these variables. Estimation of τ is possible by using precise and sophisticated measurements of the signal's travel-time. However, the values of ρ and ϕ cannot be calculated using a commercial NIC. Therefore, CRLB variance cannot be used in practice. The proposed fusion technique uses the variance of the RSSI and variance of the AoA in the PDFs. Change of the AoA variance does not have a signifi-

Table 3: Estimated position error for different variance (RMSE).

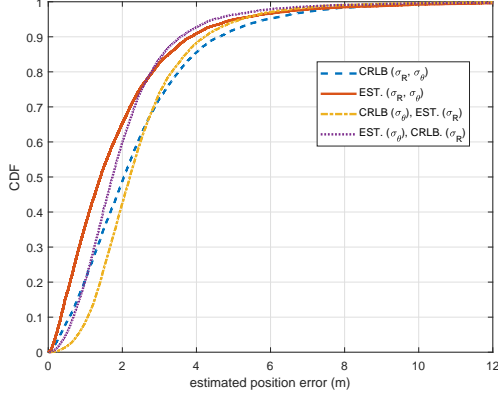|	AoA CRLB variance, $\sigma^2_{\theta,cr}$	AoA variance, $\sigma^2_{\tilde{\theta}}$
RSSI CRLB variance, $\sigma^2_{R,cr}$	2.4176 meter	2.4970 meter
RSSI variance, $\sigma^2_{\tilde{R}}$	2.0320 meter	1.8884 meter

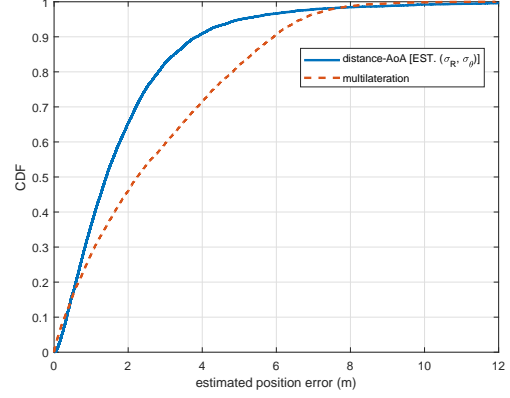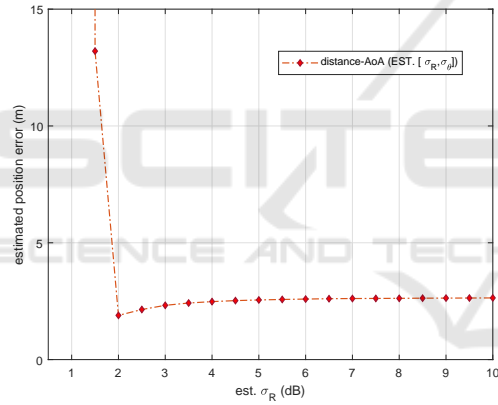Figure 4: CDF of position error of two techniques using CRLB variances.

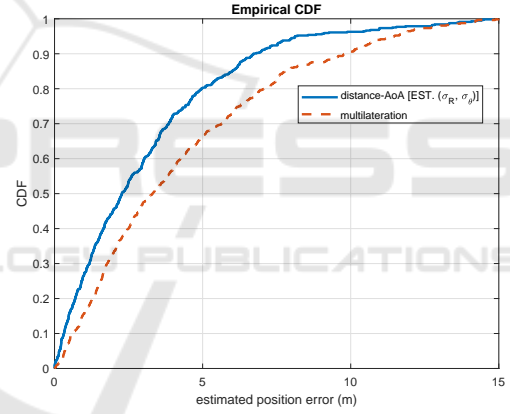
Figure 5: estimated $\sigma_{\tilde{R}}$ vs estimated position error.

Figure 6: CDF of position error of distance-AoA fusion and multilateration.

Figure 7: CDF of position error of distance-AoA fusion and multilateration for 30m×30m scenario.

cant effect on the estimation performance. However, changing the variances of RSSI from CRLB to 'measured' improves the position error by 40 cm, approximately. In Figure 5, we show an estimation performance for a range of $\sigma_{\tilde{R}}$ (RSSI STD) values. The range of $\sigma_{\tilde{R}}$ is between 0.5 dB and 10 dB with 0.5 dB steps. The position errors with $\sigma_{\tilde{R}}$ are measured as the average of RMSE for 10000 trials. For the values below 2 dB, the position error is large while it decreases rapidly at 2 dB point. After 2dB, the error graph remains almost flat until the end. In our calculations, the value of CRLB RSSI STD, $\sigma_{R,cr}$, is frequently lower than 2 dB while estimated STD, $\sigma_{\tilde{R}}$, is frequently higher than the 2 dB. It leads to a higher accuracy in position estimation using the estimated variance of RSSI. In practical scenarios, $\sigma_{\tilde{R}}$ can be measure by taking multiple RSSI measurements at a

fixed position and $\sigma_{\tilde{\theta}}$ can be measured by taking multiple AoA estimation at a fixed angle.

5.3 Comparison

The most similar technique discussed earlier estimates the location of the target node using the RSSI from both BLE and WiFi access point (Galván-Tejada et al., 2013). We implement this technique using RSSI at the WiFi access point along with RSSI received from BLE beacons. We use the multilateration technique on the calculated distance from the RSSI measurements and compare the estimation performance with our proposed fusion technique. We use the best performing combination of the variances for the proposed fusion technique. The performance

comparison is shown in Figure 6. The CDF of estimated position error reduces the RMSE of the estimated position by almost 30% from 2.7450 meters to 1.8884 meters. Figure 7 shows the CDF of estimated position error when the simulation area has been increased to 30m×30m and the number of BLE beacon has been increased to 30. The mean error of the fusion technique is 3.0883 meters and for multilateration based technique its 4.2658 meters.

6 CONCLUSION

Position estimation using RSSI has high estimation error due to its random fluctuation in the indoor environment. On the other hand, estimation of AoA using CSI data has ambiguities. In our proposed multi-radio fusion framework, we combine RSSI and CSI measurements to develop a technique that overcomes the limitation of these two wireless platforms. We used the CSI from WiFi for the first time in the fusion-based location estimation technique. CSI based techniques are complex but accurate, while RSSI based techniques are less scalable, and the localization performance vastly depends on the number and strategy of beacon deployment. From the BLE RSSI measurements, we estimate a position using the MLE solution considering the log-normal shadowing pathloss model. In WiFi, we use MMP algorithm on the CSI data to estimate the AoA. We propose a fusion technique using the RSSI and CSI measurements. We estimate an initial position using WCL to remove the ambiguities of the estimated AoA. In the fusion technique, we use the PDFs of the estimated distance and AoA. The distances are calculated using the RSSI measurements. We present a performance analysis of the fusion technique using a different combination of CRLB variances and measured variances for both distance and AoA in the PDFs. The performance analysis shows that the fusion technique performs better with both PDF using the measured variances. Moreover, the technique performs 30% better than the most similar fusion based technique using BLE and WiFi. In future work, we will investigate the prospect of integrating the information available from the neighboring WiFi access points to improve the localization accuracy.

REFERENCES

Wireless InSite - 3D Wireless Prediction Software, https://www.remcom.com/wireless-insite-em-propagation-software/. Accessed 10 Sep. 2016.

Ahmed, A., Arablouei, R., de Hoog, F., Kusy, B., Jurdak, R., and Bergmann, N. (2018). Estimating angle-of-arrival and time-of-flight for multipath components using wifi channel state information. *Sensors*, 18(6):1753.

Aparicio, S., Pérez, J., Bernardos, A. M., and Casar, J. R. (2008). A fusion method based on bluetooth and wlan technologies for indoor location. In *IEEE International Conference on Multisensor Fusion and Integration for Intelligent Systems*, pages 487–491. IEEE.

Aparicio, S., Pérez, J., Tarrío, P., Bernardos, A. M., and Casar, J. R. (2009). An indoor location method based on a fusion map using bluetooth and wlan technologies. In *International Symposium on Distributed Computing and Artificial Intelligence*, pages 702–710. Springer.

Blumenthal, J., Grossmann, R., Golatowski, F., and Timmermann, D. (2007). Weighted centroid localization in zigbee-based sensor networks. In *IEEE International Symposium on Intelligent Signal Processing*, pages 1–6. IEEE.

Büyükçorak, S., Vural, M., and Kurt, G. K. (2015). Lognormal mixture shadowing. *IEEE Transactions on Vehicular Technology*, 64(10):4386–4398.

Chan, Y. W. E. and Soong, B.-H. (2016). Discrete weighted centroid localization (dwcl): Performance analysis and optimization. *IEEE Access*, 4:6283–6294.

Chang, Q., Van de Velde, S., Wang, W., Li, Q., Hou, H., and Heidi, S. (2015). Wi-fi fingerprint positioning updated by pedestrian dead reckoning for mobile phone indoor localization. In *China Satellite Navigation Conference (CSNC) 2015 Proceedings: Volume III*, pages 729–739. Springer.

Chen, L.-H., Wu, E. H.-K., Jin, M.-H., and Chen, G.-H. (2014). Intelligent fusion of wi-fi and inertial sensor-based positioning systems for indoor pedestrian navigation. *IEEE Sensors Journal*, 14(11):4034–4042.

Choi, B.-S., Lee, J.-W., Lee, J.-J., and Park, K.-T. (2011). A hierarchical algorithm for indoor mobile robot localization using rfid sensor fusion. *IEEE Transactions on Industrial Electronics*, 58(6):2226–2235.

Dobrev, Y., Flores, S., and Vossiek, M. (2016). Multi-modal sensor fusion for indoor mobile robot pose estimation. In *IEEE/ION Position, Location and Navigation Symposium (PLANS)*, pages 553–556. IEEE.

Ergen, S. C., Tetikol, H. S., Kontik, M., Sevlian, R., Rajagopal, R., and Varaiya, P. (2014). Rssi-fingerprinting-based mobile phone localization with route constraints. *IEEE Transactions on Vehicular Technology*, 63(1):423–428.

Evennou, F. and Marx, F. (2006). Advanced integration of wifi and inertial navigation systems for indoor mobile positioning. *EURASIP journal on applied signal processing*, 2006:164–164.

Fang, L., Antsaklis, P. J., Montestruque, L. A., McMickell, M. B., Lemmon, M., Sun, Y., Fang, H., Koutroulis, I., Haenggi, M., Xie, M., et al. (2005). Design of a wireless assisted pedestrian dead reckoning system-the navmote experience. *IEEE transactions on Instrumentation and Measurement*, 54(6):2342–2358.

Gallagher, T., Wise, E., Li, B., Dempster, A. G., Rizos, C., and Ramsey-Stewart, E. (2012). Indoor positioning system based on sensor fusion for the blind and visually impaired. In *International Conference on Indoor Positioning and Indoor Navigation (IPIN)*, pages 1–9. IEEE.

Galván-Tejada, C. E., Carrasco-Jiménez, J. C., and Brena, R. F. (2013). Bluetooth-wifi based combined positioning algorithm, implementation and experimental evaluation. *Procedia Technology*, 7:37–45.

Galvan-Tejada, I., Sandoval, E. I., Brena, R., et al. (2012). Wifi bluetooth based combined positioning algorithm. *Procedia Engineering*, 35:101–108.

Gazzah, H. and Delmas, J.-P. (2012). Direction finding antenna arrays for the randomly located source. *IEEE Transactions on Signal Processing*, 60(11):6063–6068.

Gezici, S., Tian, Z., Giannakis, G. B., Kobayashi, H., Molisch, A. F., Poor, H. V., and Sahinoglu, Z. (2005). Localization via ultra-wideband radios: a look at positioning aspects for future sensor networks. *IEEE signal processing magazine*, 22(4):70–84.

Golestani, A., Petreska, N., Wilfert, D., and Zimmer, C. (2014). Improving the precision of rssi-based low-energy localization using path loss exponent estimation. In *2014 11th Workshop on Positioning, Navigation and Communication (WPNC)*, pages 1–6. IEEE.

Gu, F., Niu, J., and Duan, L. (2017). Waipo: A fusion-based collaborative indoor localization system on smartphones. *IEEE/ACM Transactions on Networking*, 25(4):2267–2280.

Gustafsson, F., Gunnarsson, F., Bergman, N., Forssell, U., Jansson, J., Karlsson, R., and Nordlund, P.-J. (2002). Particle filters for positioning, navigation, and tracking. *IEEE Transactions on signal processing*, 50(2):425–437.

Hilsenbeck, S., Bobkov, D., Schroth, G., Huitl, R., and Steinbach, E. (2014). Graph-based data fusion of pedometer and wifi measurements for mobile indoor positioning. In *Proceedings of the 2014 ACM international joint conference on pervasive and ubiquitous computing*, pages 147–158. ACM.

Hua, Y. (1992). Estimating two-dimensional frequencies by matrix enhancement and matrix pencil. *IEEE Transactions on Signal Processing*, 40(9):2267–2280.

Jacobs, E. and Ralston, E. W. (1981). Ambiguity resolution in interferometry. *IEEE Transactions on Aerospace and Electronic Systems*, (6):766–780.

Jiao, J., Li, F., Tang, W., Deng, Z., and Cao, J. (2018). A hybrid fusion of wireless signals and rgb image for indoor positioning. *International Journal of Distributed Sensor Networks*, 14(2):1550147718757664.

Kanaris, L., Kokkinis, A., Liotta, A., and Stavrou, S. (2017). Fusing bluetooth beacon data with wi-fi radiomaps for improved indoor localization. *Sensors*, 17(4):812.

Karim, L., Nasser, N., and El Salti, T. (2010). Relma: a range free localization approach using mobile anchor node for wireless sensor networks. In *Global

Telecommunications Conference (IEEE GLOBECOM 2010*, pages 1–5. IEEE.

Koo, B., Lee, S., Lee, M., Lee, D., Lee, S., and Kim, S. (2014). Pdr/fingerprinting fusion indoor location tracking using rss recovery and clustering. In *International Conference on Indoor Positioning and Indoor Navigation (IPIN)*, pages 699–704. IEEE.

Kotaru, M., Joshi, K., Bharadia, D., and Katti, S. (2015). Spotfi: Decimeter level localization using wifi. In *ACM SIGCOMM Computer Communication Review*, volume 45, pages 269–282. ACM.

Kuban, D. A., Dong, L., Cheung, R., Strom, E., and De Crevoisier, R. (2005). Ultrasound-based localization. In *Seminars in radiation oncology*, volume 15, pages 180–191. Elsevier.

Laurendeau, C. and Barbeau, M. (2009). Centroid localization of uncooperative nodes in wireless networks using a relative span weighting method. *EURASIP Journal on Wireless Communications and Networking*, 2010(1):567040.

Leppäkoski, H., Collin, J., and Takala, J. (2013). Pedestrian navigation based on inertial sensors, indoor map, and wlan signals. *Journal of Signal Processing Systems*, 71(3):287–296.

Li, Y., Zhuang, Y., Zhang, P., Lan, H., Niu, X., and El-Sheimy, N. (2017). An improved inertial/wifi/magnetic fusion structure for indoor navigation. *Information Fusion*, 34:101–119.

Lim, C.-H., Wan, Y., Ng, B.-P., and See, C.-M. S. (2007). A real-time indoor wifi localization system utilizing smart antennas. *IEEE Transactions on Consumer Electronics*, 53(2).

Lin, T., Li, L., and Lachapelle, G. (2015). Multiple sensors integration for pedestrian indoor navigation. In *International Conference on Indoor Positioning and Indoor Navigation (IPIN)*, pages 1–9. IEEE.

Liu, M., Chen, R., Li, D., Chen, Y., Guo, G., Cao, Z., and Pan, Y. (2017). Scene recognition for indoor localization using a multi-sensor fusion approach. *Sensors*, 17(12):2847.

Luo, R. C. and Chen, O. (2013). Wireless and pyroelectric sensory fusion system for indoor human/robot localization and monitoring. *IEEE/ASME Transactions on mechatronics*, 18(3):845–853.

Luo, R. C. and Lai, C. C. (2012). Enriched indoor map construction based on multisensor fusion approach for intelligent service robot. *IEEE Transactions on Industrial Electronics*, 59(8):3135–3145.

Mirowski, P., Ho, T. K., Yi, S., and MacDonald, M. (2013). Signalslam: Simultaneous localization and mapping with mixed wifi, bluetooth, lte and magnetic signals. In *International Conference on Indoor Positioning and Indoor Navigation (IPIN)*, pages 1–10. IEEE.

Nguyen, H. A., Guo, H., and Low, K.-S. (2011). Real-time estimation of sensor node's position using particle swarm optimization with log-barrier constraint. *IEEE Transactions on Instrumentation and Measurement*, 60(11):3619–3628.

Nowak, T., Hartmann, M., Zech, T., and Thielecke, J. (2016). A path loss and fading model for rssi-based

localization in forested areas. In *2016 IEEE-APS Topical Conference on Antennas and Propagation in Wireless Communications (APWC)*, pages 110–113. IEEE.

Papaioannou, S., Wen, H., Markham, A., and Trigoni, N. (2014). Fusion of radio and camera sensor data for accurate indoor positioning. In *IEEE 11th International Conference on Mobile Ad Hoc and Sensor Systems (MASS)*, pages 109–117. IEEE.

Qi, H. and Moore, J. B. (2002). Direct kalman filtering approach for gps/ins integration. *IEEE Transactions on Aerospace and Electronic Systems*, 38(2):687–693.

Seong, J.-H., Lee, S.-H., Yoon, K.-K., and Seo, D.-H. (2019). Ellipse coefficient map-based geomagnetic fingerprint considering azimuth angles. *Symmetry*, 11(5):708.

Tarrío, P., Cesana, M., Tagliasacchi, M., Redondi, A., Borsani, L., and Casar, J. R. (2011). An energy-efficient strategy for combined rss-pdr indoor localization. In *IEEE International Conference on Pervasive Computing and Communications Workshops (PERCOM Workshops)*, pages 619–624. IEEE.

Teunissen, P. (2003). Theory of carrier phase ambiguity resolution. *Wuhan University Journal of Natural Sciences*, 8(2):471.

Yiu, S., Dashti, M., Claussen, H., and Perez-Cruz, F. (2016). Locating user equipments and access points using rssi fingerprints: A gaussian process approach. In *IEEE International Conference on Communications (ICC)*, pages 1–6. IEEE.

Zanca, G., Zorzi, F., Zanella, A., and Zorzi, M. (2008). Experimental comparison of rssi-based localization algorithms for indoor wireless sensor networks. In *Proceedings of the workshop on Real-world wireless sensor networks*, pages 1–5. ACM.